NASA Technical Memorandum 81537

PREDICTION OF UNSUPPRESSED JET ENGINE EXHAUST NOISE IN FLIGHT FROM STATIC DATA

James R. Stone
Lewis Research Center
Cleveland, Ohio

Prepared for the
Sixth Aeroacoustics Conference
sponsored by the American Institute of Aeronautics and Astronautics
Hartford, Connecticut, June 4-6, 1980

NASA

PREDICTION OF UNSUPPRESSED JET ENGINE EXHAUST NOISE IN FLIGHT FROM STATIC DATA

by James. R. Stone*

National Aeronautics and Space Administration
Lewis Research Center
Cleveland, Ohio 44135

ABSTRACT

In order to assess the impact of aircraft noise on the environment in the vicinity of an airport, it is essential that a methodology be developed for predicting in-flight exhaust noise from static data. Such a methodology is presented in this paper and is compared with experimental data for several unsuppressed turbojet engines. For each engine, static data over a range of jet velocities are compared with the predicted jet mixing noise and shock-cell noise. The static engine noise over and above the jet and shock noises is identified as "excess" noise. The excess noise data are then empirically correlated to smooth the spectral and directivity relations and account for variations in test conditions. This excess noise is then projected to flight based on the assumption that the only effects of flight are a Doppler frequency shift and a level change given by 40 log $(1 - M_0 \cos \theta)$, where M_0 is the flight Mach number and θ is the observer angle relative to the jet axis. The effects of flight on jet mixing noise and shock noise are computed by published NASA methods.

E-491

INTRODUCTION

In order to assess the impact of aircraft noise on the environment in the vicinity of an airport, it is necessary to predict the effects of flight on jet engine exhaust noise. For new or proposed aircraft such predictions must often be made on the basis of only static data for the full-scale engine, since costs limit the number of configurations which can be flight tested. Therefore, it is essential that a methodology be developed for predicting in-flight exhaust noise from static data.

Some reported flight data (e.g., refs. 1 and 2) on jet engine exhaust noise did not agree with projections based on classical theory or flight simulation experiments. The in-flight levels were found to exceed the extrapolated static levels over a wide range of angles, particularly in the forward quadrant. It was subsequently shown (ref. 3) that these apparently anomalous flight effects can be largely reconciled on the basis of the combined contributions of jet mixing noise and internally-generated exhaust noise. The agreement is further improved when the distributed nature of the jet mixing noise source region is taken into account in the extrapolation of the static data (ref. 4). In certain cases installation effects, such as thick nacelle boundary layers (ref. 5) and interaction with airframe structures (refs. 6 and 7), may become important.

*Head, Section A, Jet Acoustics Branch; AIAA Member.

More recently reported flight tests (e.g., refs. 4 and 7 to 10) showed a wide range of results. In some cases an in-flight noise increase in the forward quadrant was observed, while in other cases in-flight noise reductions were observed at all angles. The forward quadrant noise increase was attributed in some cases to internally-generated noise (ref. 8) or shock noise (ref. 10).

It was subsequently demonstrated (ref. 11) that static and in-flight exhaust noise could be predicted with reasonable accuracy when the multiple-source nature of the problem is taken into account. The agreement of this approach with experimental data was good for jet velocities up to about 520 m/sec. The poorer agreement at higher jet velocities appeared to be due primarily to the manner in which supersonic convection effects were formulated. The purely empirical supersonic convection formulation of reference 11 was then replaced by one based on theoretical considerations (refs. 12 and 13). This revised method was shown (ref. 14) to predict static-to-flight jet noise increments to a standard deviation of 1.5 dB for turbojet and turbofan engines. This same approach was then incorporated into a static and flight jet-mixing and shock noise prediction procedure and verified by comparisons with model-scale static and simulated-flight data in reference 15.

It is the purpose of this paper to present and verify a methodology for predicting in-flight exhaust noise from static data for unsuppressed turbojet engines and to illustrate the application of this method to turbofan engines. For each engine, static data over a range of jet velocities are compared with the predicted jet mixing noise and shock-cell noise from reference 15. The static engine noise over and above the predicted jet and shock noises is identified as "excess" noise. The excess noise data are then empirically correlated to smooth the spectral and directivity relations and account for variations in test conditions. This empirically correlated excess noise is then projected to flight based on the assumption that the only effects of flight are a Doppler frequency shift and a level change given by $40 \log (1 - M_0 \cos \theta)$, where M_0 is the flight Mach number and θ is the observer angle relative to the inlet axis. The effects of flight on jet mixing noise and jet shock noise are computed by published NASA Lewis methods (refs. 14 and 15). Installation effects are not included since these are thought to be unique for each installation but not of significant magnitude for any of the cases considered herein. It should be noted that the so-called "excess" noise may include some jet and/or shock noise under-predicted from reference 15 as well as noise from other engine sources. The methodology proposed in this paper projects all of the excess noise to flight using the above flight effects rather than adjusting the prediction procedures. This may produce some inaccuracies, due to the differences in flight effects between jet noise and the other sources. But it is felt that these inaccuracies are small and acceptable in view of the simplification of not having to make a judgement as to the nature of the excess noise.

SYMBOLS

(All symbols are in S.I. units unless noted)

A	area
c	speed of sound

f	1/3-octave-band center frequency
F_S	frequency shift parameter for coaxial jets (eq. (5))
M	Mach number, V/c
m	coaxial jet exponent (eq. (4))
OASPL	overall sound pressure level, dB re 20 $\mu N/m^2$
SPL	1/3-octave-band sound pressure level, dB re 20 $\mu N/m^2$
T	total temperature
V	velocity
β	effective engine angle of attack (fig. 2), deg
θ	polar angle from inlet axis (fig. 2), deg

Subscripts:

a	ambient
C	core noise
E	excess noise
F	flight
j	fully-expanded jet
o	aircraft
S	static
1	inner stream (primary)
2	outer stream (secondary)
90°	evaluated at $\theta = 90°$

METHODOLOGY

The methodology of the present method is illustrated in figure 1. The experimentally-determined static total noise is compared with the jet mixing and shock noise predicted according to reference 15. The predicted jet mixing noise and shock noise are antilogarithmically subtracted from the total measured noise to produce an inferred excess noise. The inferred excess noise is correlated with similar data for other angles and power settings to produce an empirical excess noise correlation. Details of the excess noise correlations are given in appendix A. The correlated excess noise and the shock noise are then projected to flight assuming a doppler frequency shift,

$$\frac{f_F}{f_S} = \frac{1}{1 - M_o \cos(\theta + \beta)} \tag{1}$$

and an amplification,

$$\Delta SPL_E = -40 \log [1 - M_o \cos(\theta + \beta)] \tag{2}$$

The jet mixing noise is predicted according to reference 15, which includes the static-to-flight increment relation of reference 14. The total projected flight noise is then obtained by logarithmic addition. For both the static and flight cases, the jet mixing and shock noise predictions include source position corrections, while the excess noise is assumed to radiate from the center of the nozzle exit plane. No other assumptions are made about the nature of the excess noise except that its flight effects are as given in equations (1) and (2).

COMPARISONS WITH TURBOJET DATA

Comparisons are made with vehicles powered by single turbojet engines in motion with vehicle Mach number M_0. The flight geometry is illustrated and some of the important variables defined in figure 2. Comparisons are presented for the F-86 airplane powered by an Orenda engine and for the Bertin Aerotrain powered by a J85 engine. In each case spectral comparisons are shown at three angles: in the forward quadrant ($\theta \cong 50°$), where shock noise becomes important at supersonic jet conditions; at $\theta \cong 90°$ (overhead), where dynamic effects are minimized; and at the peak noise angle ($\theta \cong 130°$) in the rear quadrant. Overall sound pressure level directivity comparisons are also shown.

F-86/Orenda

The Boeing Company conducted static and flyover noise tests on an F-86 airplane powered by an Orenda turbojet engine (ref. 16). The results of these tests were subsequently made available to NASA to increase the available data base for turbojet engine exhaust noise flight effects. Static tests were conducted with ground microphones placed on a 29-m arc in the forward quadrant and on a 29-m sideline in the rear quadrant. Inlet noise was shielded from the microphones by barrier boards. The results reported by Strout (ref. 16) were corrected for source position using methods developed from multiple-sideline noise measurements by Jaeck (ref. 17). (Therefore, no source position corrections are needed for this case.) Flight data were obtained from multiple ground microphones for level 61-m flyovers at flight Mach numbers, M_0, of about 0.34 and jet velocities, V_j, of 335, 498, and 596 m/sec. Static data were obtained at these conditions as well as at conditions producing the same relative velocities, $V_j - V_0$, as the flight cases. Since the inlet noise barrier could not be used in flight, some contamination of the results by inlet radiated noise is present. The comparisons shown herein are at constant absolute jet velocity, V_j, while the other static data were used to help establish the excess noise correlation. It should be noted that the data obtained at other angles than those illustrated herein were also analyzed to develop the excess noise correlation.

Forward quadrant. - Experimental and predicted spectra for an angle, θ, of 50° are shown in figure 3. In each case, the experimental SPL, denoted by an appropriate symbol, should be compared with the predicted total noise (solid curve). Note that since the empirically-correlated excess noise is used, the agreement between the individual static data points and the prediction is not exact. Static comparisons are shown in figure 3(a). At the highest jet velocity, V_j = 596 m/sec, shock noise is the most important noise source in terms of OASPL, while jet mixing noise is dominant at low frequencies. At lower jet velocities, jet mixing noise is dominant except at high frequencies where the excess noise may be emanating from the turbomachinery. The excess noise, while not dominant, does contribute significantly in the middle and high frequency range.

The corresponding flight comparisons are shown in figure 3(b). The main difference between the static and flight cases is that jet mixing noise is less important in flight, with the excess noise being dominant at frequencies of 200 to 400 Hz or more. At the highest jet velocity, the shock noise is dominant at frequencies above 630 Hz. In general, the agreement of

the experimental data with the total noise projection is good except for the lowest jet velocity, where a narrow-band low frequency source is not adequately accounted for.

Overhead. - Experimental and predicted spectra for an angle, θ, of 90° are shown in figure 4. Static comparisons are shown in figure 4(a). Jet mixing noise is dominant except at the lowest jet velocity, where significant high-frequency excess noise appears and at the highest jet velocity, where shock noise is dominant at frequencies above 1250 Hz. Excess noise again contributes to the SPL values at middle and high frequencies. In flight (fig. 4(b)), the jet mixing noise relative contribution is reduced, but it is still the dominant source at low frequencies. At the highest jet velocity shock noise is the dominant source, while at low jet velocity the excess noise is dominant; for the intermediate jet velocity, jet mixing and excess noise both contribute significantly to the middle and high frequency range. In general, the spectral agreement is rather good near the peak. The disagreement at high frequencies for the subsonic conditions may be at least partially due to the use of an inlet noise barrier during the static tests.

Peak noise angle. - Experimental and predicted spectra are shown in figure 5 for an angle, θ, of 130° which is at or near the angle of peak noise in flight. Static comparisons are shown in figure 5(a). At this angle, jet mixing noise and excess noise both contribute substantially, and shock noise is not significant. In flight (fig. 5(b)), excess noise is the strongest noise source. There is apparently some under-prediction of the jet mixing noise under both static and flight conditions, but the general agreement is still reasonably good.

OASPL directivity. - Experimental and predicted OASPL directivities are shown in figure 6. As with the spectral comparisons, the experimental value, denoted by an appropriate symbol, should be compared with the predicted total noise (solid curve). Static comparisons are shown in figure 6(a). Jet mixing noise controls the peak noise at the highest jet velocity, while at the lower jet velocities, excess noise makes a nearly equal contribution. In the forward quadrant, the jet noise is generally higher than the excess noise, while at the highest jet velocity shock noise is dominant up to near 80°. Because the empirically-correlated excess noise is used, the agreement between individual static data points and the prediction is not exact, leading to a standard deviation of 1.6 dB and an average overprediction of 0.9 dB.

The corresponding flight comparisons are shown in figure 6(b). The relative importance of jet mixing noise is reduced in flight; even at the highest jet velocity, excess noise appears to be dominant at the peak noise angle. Furthermore, shock noise dominates the forward quadrant at high jet velocity. Excess noise is almost completely dominant at the lowest jet velocity and is controlling for angles forward of 140° at the intermediate jet velocity. In general, the agreement between experimental and predicted values is quite good, with a standard deviation of 1.7 dB and an average overprediction of less than 0.1 dB. The results and the spectral comparisons indicate that in-flight noise levels can be projected with reasonable accuracy from static data.

As a part of the FAA/DOT sponsored high velocity jet noise reduction program, the General Electric Company conducted static and simulated-flight tests on the Bertin Aerotrain powered by a J85 engine (ref. 18). The static and flight data were obtained from the same 50-m sideline microphone array. The static data were obtained by creeping the tracked air-cushion vehicle past the microphones. Because of this simplification, the source position corrections, which are fairly small (<1.6° and <0.1 dB), are the same for both static and flight data. Data were obtained for vehicle Mach numbers, M_0, of 0.12 and 0.24, but only the higher M_0 data are considered herein. Comparisons are made at three nominal jet velocities, 460, 564 and 670 m/sec.

Forward quadrant. - Experimental and predicted spectra for an angle, θ, of 49° are shown in figure 7. Static comparisons are shown in figure 7(a). At the highest jet velocity (V_j = 687 ft/sec) shock noise is the most important contributor in terms of OASPL, while excess noise is dominant at low frequencies. At the intermediate jet velocity (V_j = 564 m/sec) excess noise dominates the low frequencies, while jet, shock and excess noises all contribute substantially in the high frequency range. (It is believed that the low frequency data at the intermediate jet velocity are somewhat high, since the levels reported exceed those of the highest jet velocity from 50-100 Hz.) At the lowest jet velocity (V_j = 451 m/sec) excess noise is dominant across most of the spectrum, with the contribution of jet mixing noise being greatest at middle to high frequencies. In motion (fig. 7(b)) the qualitative effects are similar, except that the relative contribution of jet mixing noise is reduced. The agreement of the "flight" data with the prediction is quite good in both level and spectral shape.

Overhead. - Experimental and predicted spectra for an angle, θ, of 88° are shown in figure 8. Static comparsions are shown in figure 8(a). At the highest jet velocity, shock noise is controlling at high frequency while jet noise is slightly stronger than excess noise over most of the middle and low frequency range. At the intermediate and low jet velocities, the contributions of jet and excess noises are close over most of the frequency range. In flight (fig. 8(b)), the excess noise contributes about as much as jet mixing noise at the highest jet velocity, but shock noise controls the high frequency range and is dominant in terms of OASPL. At the intermediate and lower jet velocities, excess noise contributes more strongly than jet mixing noise. The spectral agreement is quite good at the intermediate and lower jet velocities, while at the highest jet velocity, there is an underprediction of the middle frequency range.

Peak noise angle. - Experimental and predicted spectra are shown in figure 9 for an angle, θ, of 129° which is at or near the peak noise angle in flight. Static comparisons are shown in figure 9(a). Shock noise is no longer predicted to be an important contributor, even at the highest jet velocity. However, any shock noise which may be present in the static data at intermediate and high jet velocities would be included in the flight prediction as excess noise at high frequency. Over this jet velocity range, both jet mixing noise and excess noise contribute substantially. In flight (fig. 9(b)), excess noise is almost totally dominant. The general agreement of the prediction with the experimental data is reasonable, but further improvements in the jet mixing noise prediction, particularly the convection model, might produce even greater accuracy.

OASPL directivity. - Experimental and predicted OASPL directivities are shown in figure 10. Static comparisons are shown in figure 10(a). At high jet velocity, jet mixing noise is the most important source at the peak noise angle, but excess noise contributes substantially. At the highest jet velocity, shock noise is controlling in the forward quadrant. At the intermediate velocity, excess and jet mixing noise both contribute substantially, while at the lowest jet velocity, excess noise is dominant up to 150°. As for the F86/Orenda (fig. 6(a)), the agreement between individual static data points and the prediction is not exact since the empirically-determined excess noise is used, leading to a standard deviation of 1.1 dB.

The corresponding flight comparisons are shown in figure 10(b). As for the F86/Orenda (fig. 6(b)), the relative importance of jet mixing noise is reduced in flight. The agreement between experimental and predicted OASPL's is good at the intermediate and high jet velocities, with a standard deviation of 1.7 dB and an average underprediction of 0.1 dB. However, the low jet velocity comparison is not very good, with an average over-prediction of 3.2 dB. But even so, for the low-V_j data within 10 dB of the peak, the average over-prediction is reduced to 2.4 dB and the standard deviation from this mean bias is 1.6 dB.

APPLICATION TO TURBOFAN ENGINES

Static-to-flight jet mixing noise increments predicted by the same method as used herein were shown in reference 14 to agree well (1.6 dB standard deviation) with experimental data for the turbofan engines on the DC-9 and DC-10 airplanes. These predictions are based on the assumption that flight effects are determined by primary stream and ambient conditions with the effect of the secondary stream being the same in flight as under static conditions. To apply the presently proposed methodology to turbofan engines on an absolute basis, it is necessary to quantify the effect of the secondary stream on level and peak frequency.

Olsen and Friedman (ref. 19) have correlated shock-free cold-flow coaxial jet noise data for secondary-to-primary jet velocity ratios, $V_{j,2}/V_{j,1}$, from 0.2 to 1 and secondary-to-primary area ratios, $A_{j,2}/A_{j,1}$, from 0.67 to 43.5. This correlation (ref. 19) is based on extension and modification of the method of Williams, et al. (ref. 20). The method of reference 19 was modified and extended to account for the case of a heated, shock-free primary jet, taking into consideration the data of Eldred (ref. 21). The approach developed in reference 22 and used herein is as follows: (1) The OASPL and the spectra at $\theta = 90°$ are related to those of the core jet alone by means of simple correlation factors; and (2) the directivity relative to $\theta = 90°$ is taken to be the same as for the primary jet alone, as the experiments had indicated. Olsen and Friedman (ref. 19) found no significant differences when the core nozzle was extended beyond the secondary nozzle exit.

Overall Sound Pressure Level

The effects of area ratio, velocity ratio, and temperature ratio are shown in figure 11, where the OASPL relative to that of the core jet alone, corrected for temperature ratio,

$$OASPL_{90^\circ} - OASPL_{90^\circ,1} - 10 \log \sqrt{\frac{T_{j,1}}{T_{j,2}}}$$

is plotted against area ratio for various velocity ratios. The temperature ratio term is an approximation. The curves shown correspond to the recommended relation of reference 22 (slightly modified from ref. 19),

$$OASPL_{90^\circ} - OASPL_{90^\circ,1} = 5 \log\left(\frac{T_{j,1}}{T_{j,2}}\right) + 10 \log\left[\left(1 - \frac{V_{j,2}}{V_{j,1}}\right)^m + 1.2 \frac{\left(1 + \frac{A_{j,2}V_{j,2}^2}{A_{j,1}V_{j,1}^2}\right)^4}{\left(1 + \frac{A_{j,2}}{A_{j,1}}\right)^3}\right] \tag{3}$$

In equation (3), $OASPL_{90^\circ,1}$ is the OASPL at $\theta = 90^\circ$ for the core jet alone from reference 15 for a circular primary nozzle. The exponent m is given by

$$m = 1.1 \sqrt{\frac{A_{j,2}}{A_{j,1}}}; \quad \frac{A_{j,2}}{A_{j,1}} < 29.7, \text{ or } \quad m = 6.0; \quad \frac{A_{j,2}}{A_{j,1}} \geq 29.7 \tag{4}$$

The ambient temperature data of reference 19 are within approximately ±2 dB of the curves shown, with the greatest scatter at a velocity ratio, $V_{j,2}/V_{j,1}$, of about 0.6.

SPL Spectra

The shapes of the SPL spectra for shock-free coaxial jets were generally found in reference 19 to be the same as for a circular nozzle, but with the frequencies shifted. Figure 12 shows the effect of area ratio and velocity ratio on the frequency shift parameter.

$$F_S = \left(1 - \frac{f_1}{f}\right)\left(\frac{T_{j,1}}{T_{j,2}}\right) \tag{5}$$

where f_1 is the peak-SPL frequency for the primary nozzle alone, and the temperature ratio term is an interim approximation.

The recommended curves in figure 12 are based on the ambient temperature data of reference 19 at $\theta = 90^\circ$ and $V_{j,1}/c_a \approx 0.87$; however, data for other angles and core jet velocities show similar trends. These data scatter within a frequency range of ±1 1/3-octave band from the curves for area ratios, $A_{j,2}/A_{j,1}$, up to 16.

Verification

This method, in conjunction with an earlier circular jet noise prediction (modified only slightly from ref. 22) was shown in reference 11 to agree well static and flight exhaust noise data for refanned JT8D engines on a DC-9 airplane. OASPL directivity comparisons of that method with the data of reference 8 are shown in figure 13 as an example. The circular jet prediction of reference 22 does not differ greatly from that used herein (ref. 15) over the range of velocities given in figure 13. Therefore, good agreement of the present approach with experimental data is expected but has not yet been documented. It is possible, however, that with increasing bypass ratio, the assumption that the effect of the secondary stream is the same for both static and flight cases may have to be modified.

CONCLUDING REMARKS

A method has been developed for predicting in-flight jet engine exhaust noise from static data. This method is demonstrated in the present paper to agree resonably well with turbojet engine data. Specifically, this method is shown to predict the in-flight OASPL directivity to within a 1.7-dB standard deviation for the Orenda engine in a F86 airplane and for the J85 engine in the Bertin Aerotrain, except at low jet velocity for the Aerotrain, where the flight noise is overpredicted by an average of 3.2 dB. The relationships required to apply this method to turbofan engines are also presented along with evidence that the method will give good results; a detailed verification has not yet been conducted for turbofans. In summary, it appears that reasonably accurate projections of jet engine exhaust noise in flight from static data can be obtained if the noise in excess of jet mixing noise statically is projected to flight on the basis of a simple dynamic effect.

APPENDIX A

EXCESS NOISE CORRELATIONS

The excess noise correlations used herein for the F-86/Orenda and the Aerotrain/J85 are shown in figures 14 and 15, respectively. The symbols represent the experimentally determined excess noise, while the curves indicate the correlated values used for projection to flight. Experimental data for other angles, and for the F-86/Orenda other jet velocities, were also used in developing these correlations. Where reasonable accuracy could be obtained by so doing, the broadband noise was assumed to vary in a manner predicted by core noise relations (refs. 3 or 11, as appropriate). This approach appears appropriate at ~50° and ~90°, but not at ~130°. It may be that this is due to an inaccuracy in the jet noise prediction at ~130°.

REFERENCES

1. Brooks, J. R. and Woodrow, R. J., "The Effects of Forward Speed on a Number of Turbojet Exhaust Silencers," AIAA Paper 75-506, Mar. 1975.

2. Bushell, K. W., "Measurement and Prediction of Jet Noise in Flight," AIAA Paper 75-461, Mar. 1975.

3. Stone, J. R., "On the Effects of Flight on Jet Engine Exhaust Noise," NASA TM X-71819, 1975.

4. Munoz, L. F., "727/JT8D Jet and Fan Noise Flight Effects Study," Boeing Commercial Airplane Co., Seattle, WA, D6-44145, Aug. 1976. (FAA-RD-76-110, AD-A031877/4)

5. Sarohia, V. and Massier, P. F., "Effects of External Boundary Layer Flow on Jet Noise in Flight," AIAA Paper 76-558, July 1976.

6. Way, D. J., "An Experimental Study of the Influence of Flight-Stream Turbulence on Jet Mixing Noise," AIAA Paper 79-0617, Mar. 1979.

7. Brooks, J. R., "Flight Noise Studies on a Turbojet Using Microphones Mounted on a 450 Ft. Tower," AIAA Paper 77-1325, Oct. 1977.

8. Merriman, J. E., Good, R. C., Low, J. K. C., Yee, P. M., and Blankenship, G. L., "Forward Motion and Installation Effects on Engine Noise," AIAA 76-584, July 1976.

9. Clapper, W. S., and Stringas, E. J., "High Velocity Jet Noise Source Location and Reduction; Task 4 - Development/Evaluation of Techniques for 'Inflight' Investigation," General Electric Co., Cincinnati, OH, R77AEG189, Feb. 1977. (FAA-RD-76-79-4, AD-A041849)

10. Drevet, P., Duponchel, J. P., and Jacques, J. R., "Effect of Flight on the Noise from a Convergent Nozzle as Observed on the Bertin Aerotrain," AIAA Paper 76-557, July 1976.

11. Stone, J. R., "Prediction of In-Flight Exhaust Noise for Turbojet and Turbofan Engines," Noise Control Engineering, Vol. 10, Jan.-Feb. 1978, pp. 40-46.

12. Ffowcs Williams, J. E., "The Noise from Turbulence Convected at High Speed," Philosophical Transactions of the Royal Society (London), Ser. A, Vol. 255, Apr. 1963, pp. 469-503.

13. Goldstein, M. E., and Howes, W. L., "New Aspects of Subsonic Aerodynamic Noise Theory," NASA TN D-7158, 1973.

14. Stone, J. R., "An Improved Method for Predicting the Effects of Flight on Jet Mixing Noise," NASA TM-79155, 1979.

15. Stone, J. R., and Montegani, F. J., "An Imroved Prediction Method for the Noise Generated in Flight by Circular Jets," NASA TM-81470, 1980.

16. Strout, F. G., "Flight Effects on Uniform Flow Jet Noise," Boeing Commercial Airplane Co., Seattle, WA, D6-48036, 1978.

17. Jaeck, C. L., "Static Wind-Tunnel Near-Field/Far-Field Jet Noise Measurements from Model Scale Single-Flow Baseline and Suppressor Nozzles, Vol. I: Noise Source Locations and Extrapolation of Static Free-Field Jet Noise Data," Boeing Commerical Airplane Co., Seattle, WA, D6-44121-1-VOL-1, Sep. 1976. (NASA CR-137913.)

18. Clapper, W., et al., "High Velocity Jet Noise Source Location and Reduction, Task 4 - Development/Evaluation of Techniques for "Inflight" Investigation," General Electric Co., Cincinnati, Ohio, R77AEG189, Feb. 1977. (FAA-RD-76-79-4; AD-A 041849.)

19. Olsen, W. A., and Friedman, R., "Jet Noise From Coaxial Nozzles Over a Wide Range of Geometric and Flow Parameters," AIAA Paper 74-43, Jan. 1974.

20. Williams, T. J., Ali, M.R.M.H., and Anderson, J. S., "Noise and Flow Characteristics of Coaxial Jets," Journal of Mechanical Engineering Science, Vol. 11, Apr. 1969, pp. 133-142.

21. Eldred, K. M., "Far Field Noise Generation by Coaxial Flow Jet Exhausts, Volume I - Detailed Discussion," Wyle Labs., Inc., El Segundo, CA, Nov. 1971. (FAA-RD-71-101-Vol-1).

22. Stone, J. R., "Interim Prediction Method for Jet Noise," NASA TM X-71618, 1974.

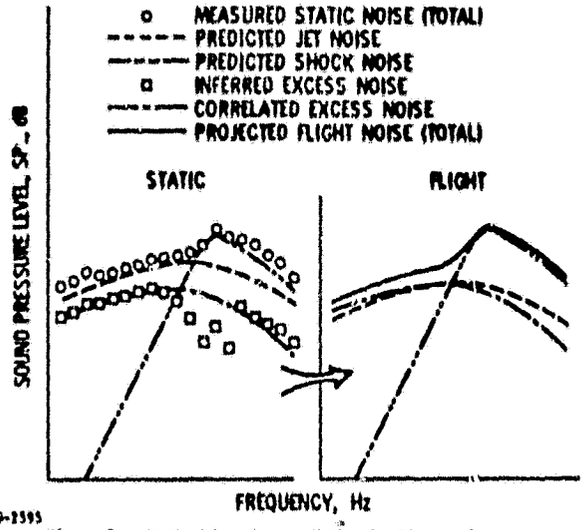

Figure 1. - Methodology for predicting in-flight noise from static data.

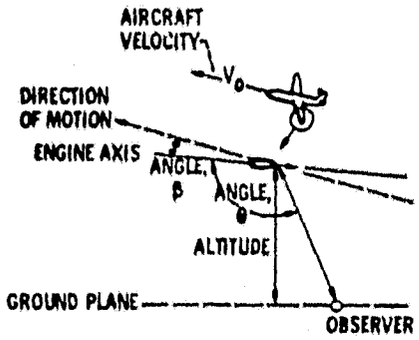

(a) GEOMETRIC PARAMETERS.

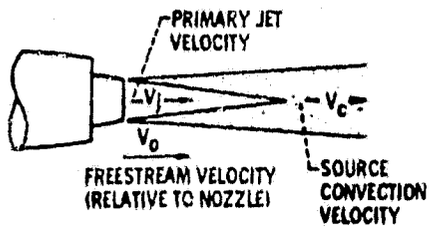

(b) JET PARAMETERS.

Figure 2. - Flight effects on jet noise: terminology for level flyover at aircraft Mach number M_0.

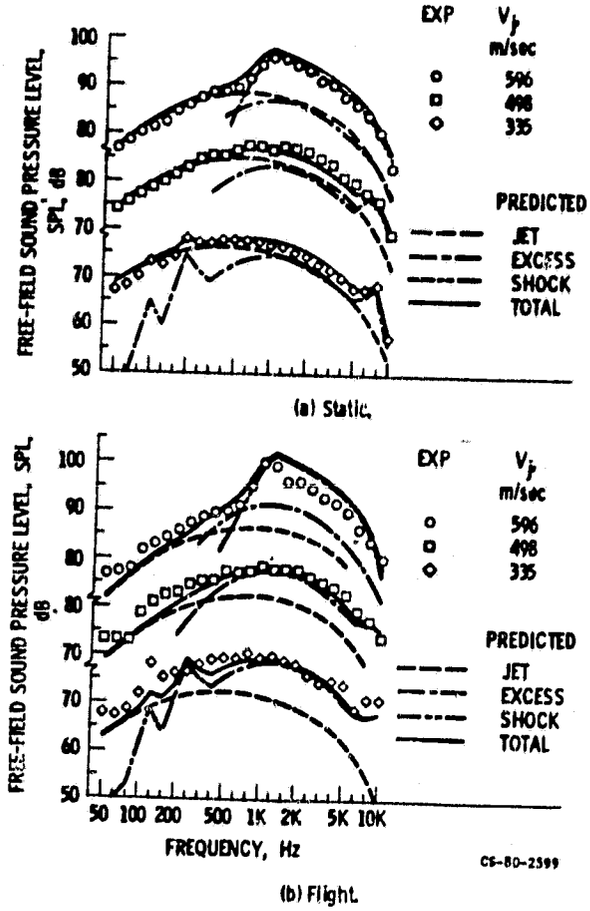

(a) Static.

(b) Flight.

Figure 3. - Experimental and predicted spectra at $\theta' = 50^0$ for Orenda turbojet on F-86 airplane.

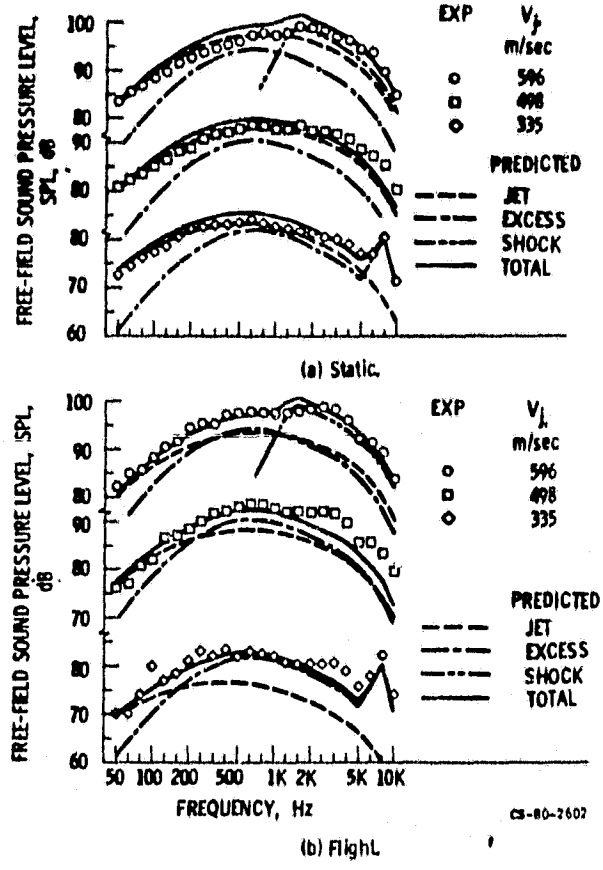

Figure 4. - Experimental and predicted spectra at $\theta = 90^0$ for Orenda turbojet on F-86 airplane.

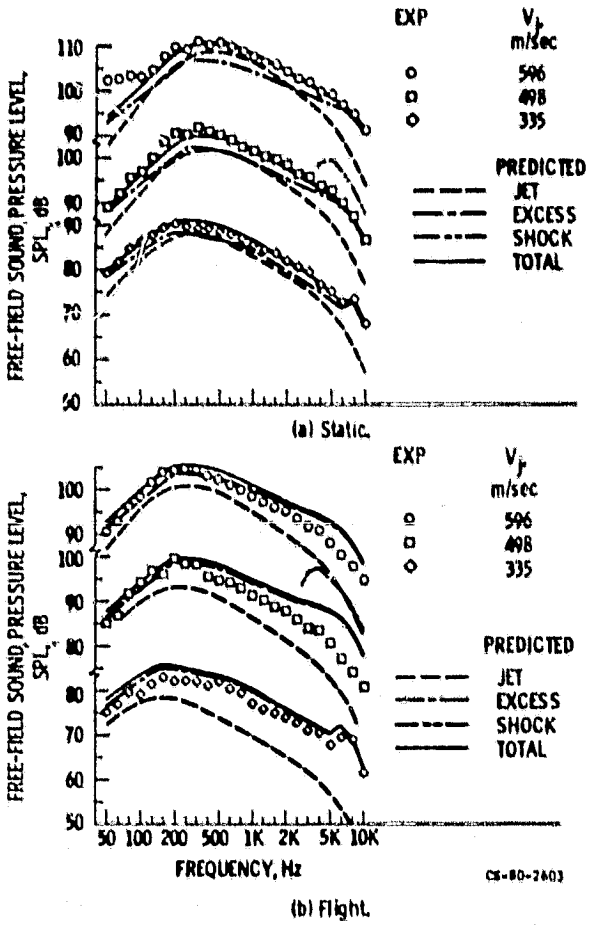

Figure 5. - Experimental and predicted spectra at $\theta = 130^0$ for Orenda turbojet on F-86 airplane.

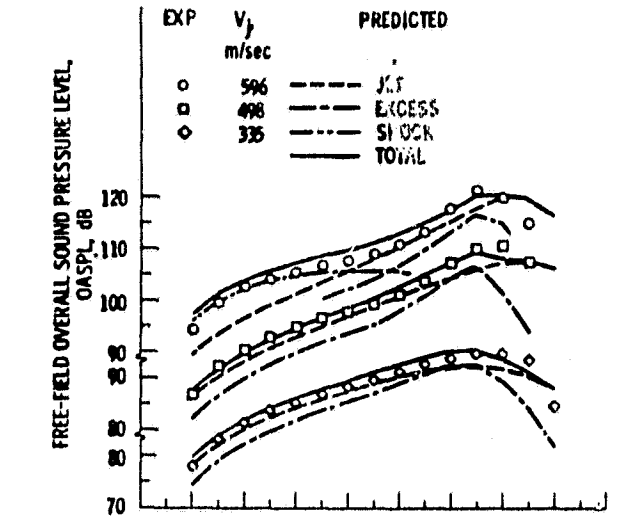

(a) Static.

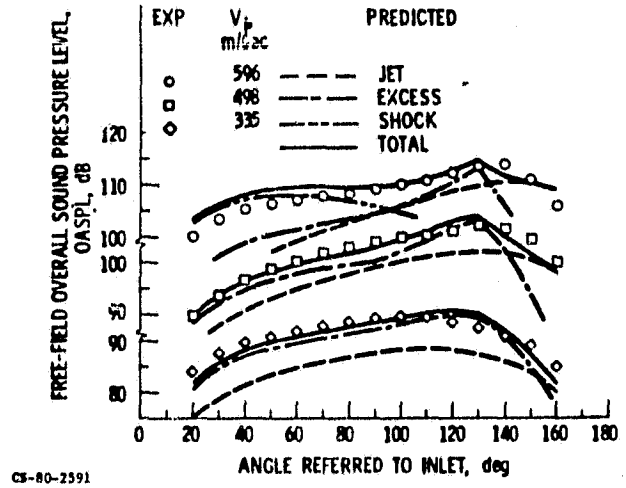

CS-80-2591

(b) Flight.

Figure 6. - Experimental and predicted OASPL directivities for Orenda turbojet in F-86 airplane.

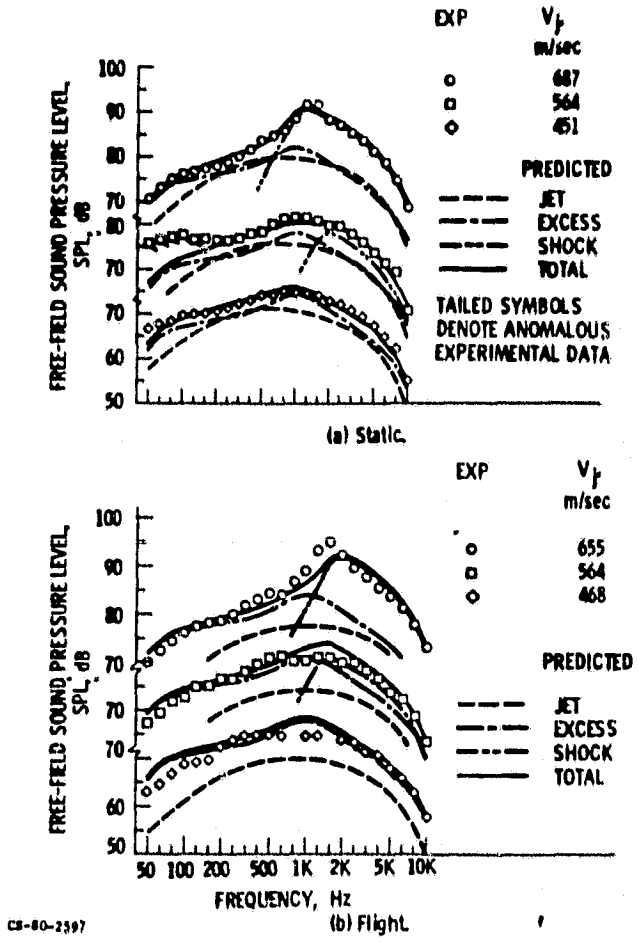

Figure 7. - Experimental and predicted spectra at $\theta = 49^0$ for J85 turbojet in Aerotrain.

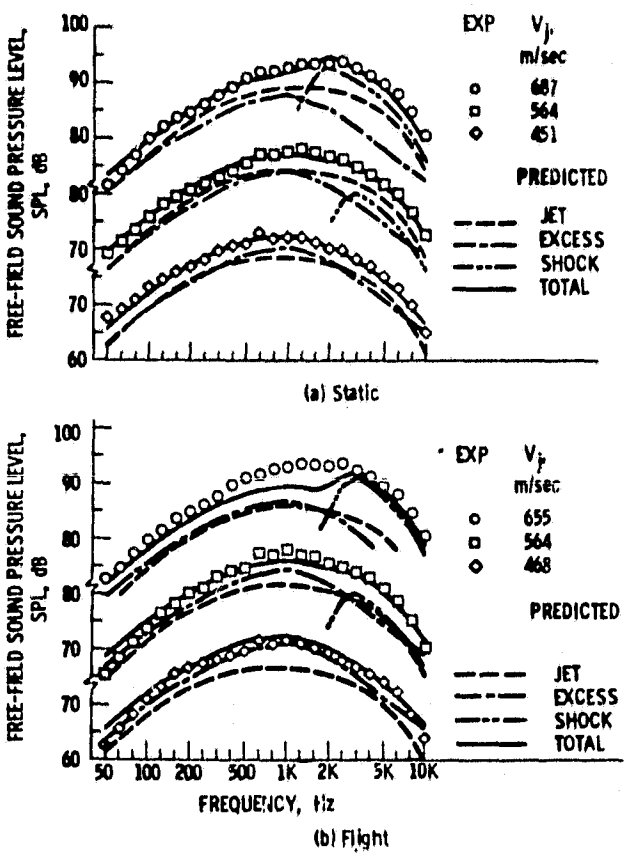

Figure 8. - Experimental and predicted spectra at $\theta = 88^{\circ}$ for J85 turbojet in Aerotrain.

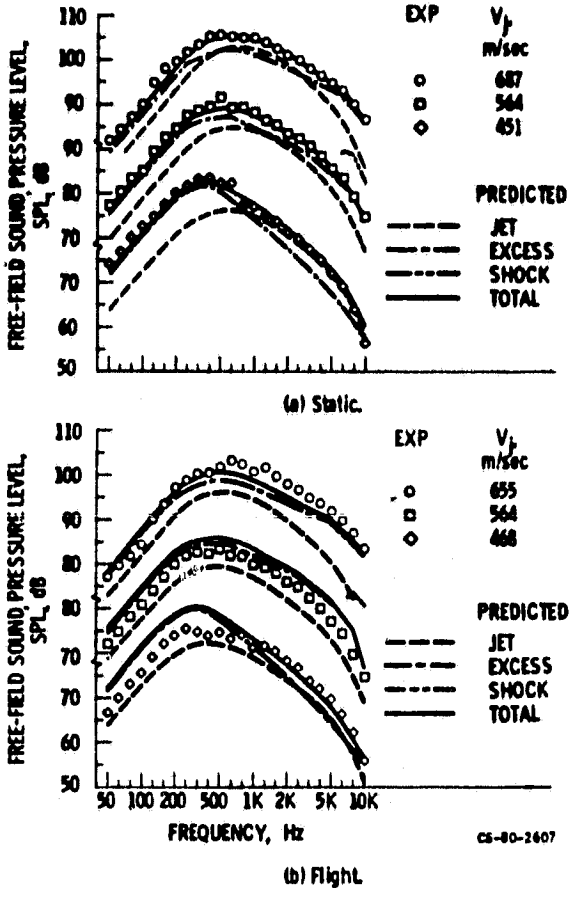

Figure 9. - Experimental and predicted spectra at $\theta = 129^{0}$ for J85 turbojet in aerotrain.

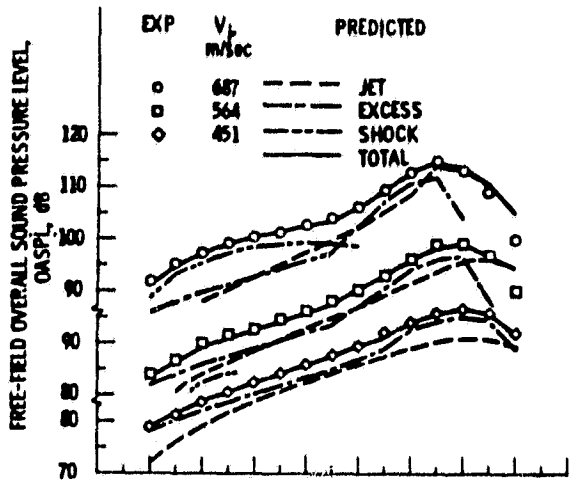

(a) Static.

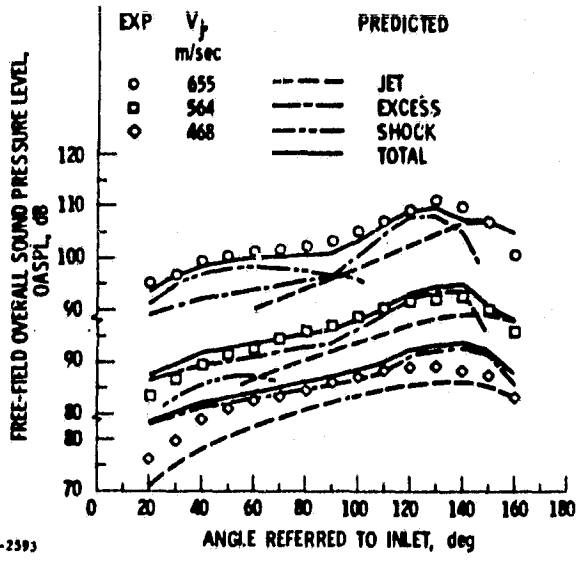

CE-80-2393

(b) Flight.

Figure 10. - Experimental and predicted OASPL directivities for J85 turbojet in Aerotrain.

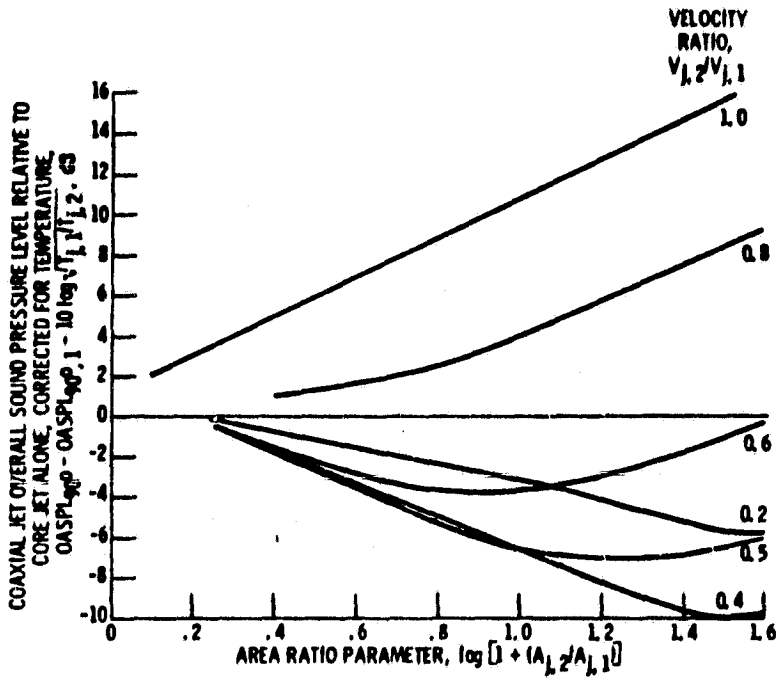

Figure 11. - Recommended prediction for coaxial jet OASPL relative to primary jet, based on extension of the method of Olsen and Friedman (ref. 19), equation (3).

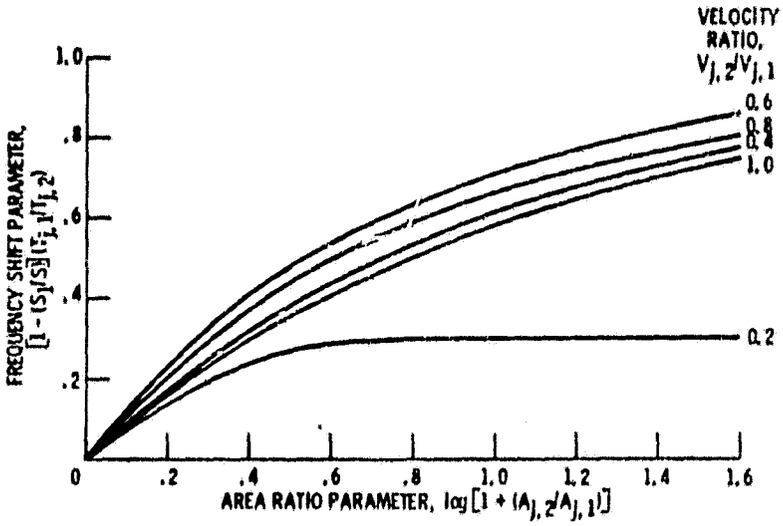

Figure 12. - Recommended frequency shift parameter for coaxial jets with respect to the primary jet, based on extension of the method of Olsen and Friedman (ref. 19).

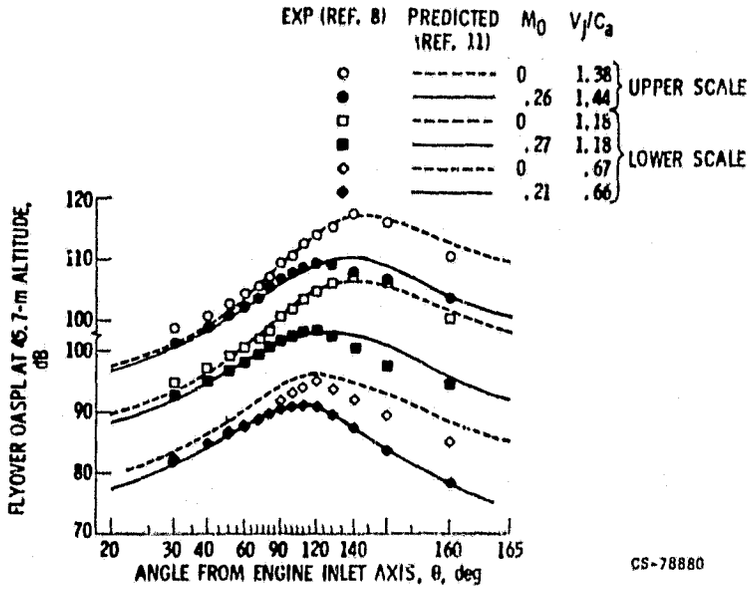

Figure 13. - Comparison of flyover and static OASPL directivities with earlier prediction (ref. 11) for refanned JT8D engines on DC-9 airplane.

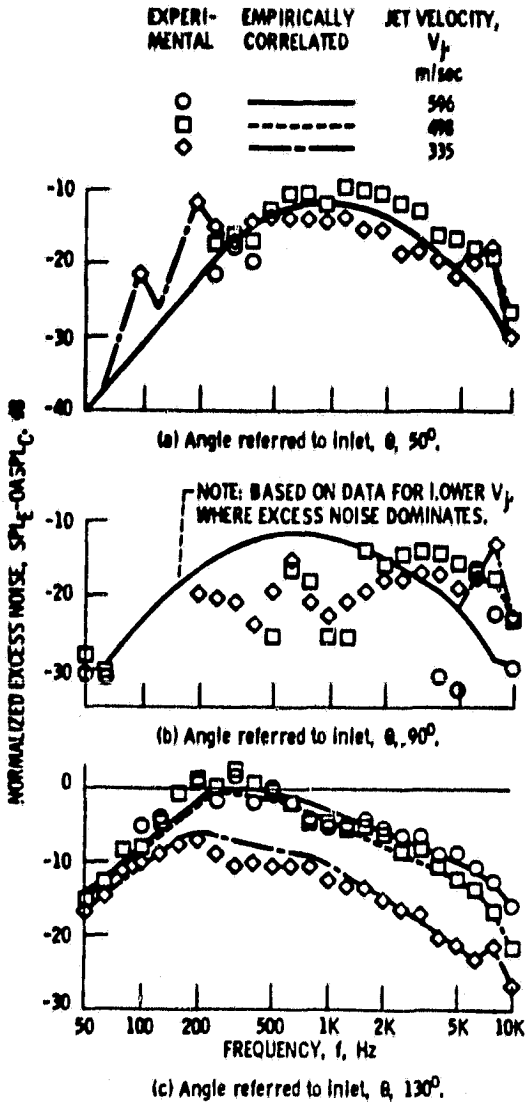

(a) Angle referred to inlet, θ, 50°.

(b) Angle referred to inlet, θ, 90°.

(c) Angle referred to inlet, θ, 130°.

Figure 14. - Experimental and empirically correlated static excess noise for Orenda turbojet on F-86 airplane.

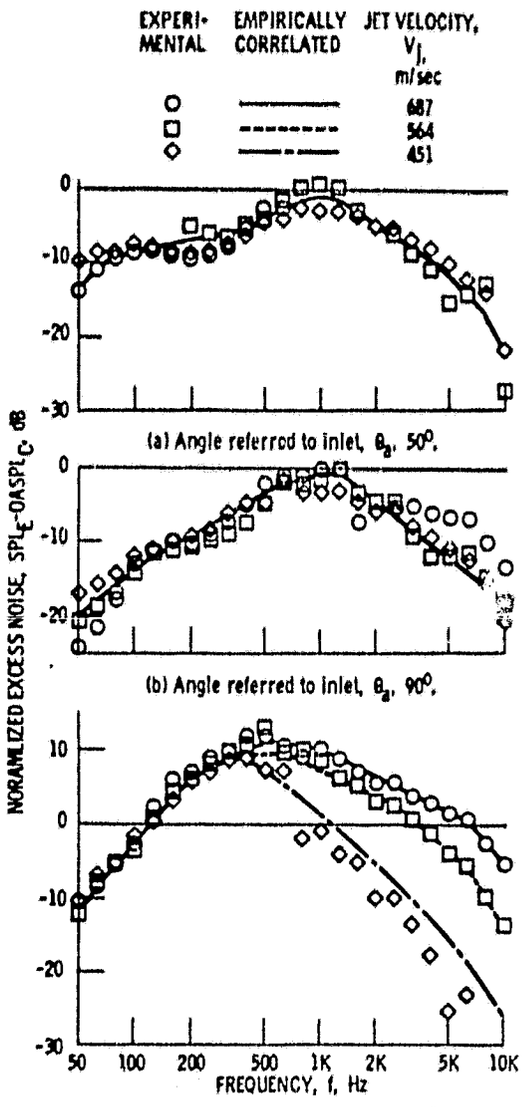

Figure 15. - Experimental and empirically correlated static excess noise for J85 turbojet on Aerotrain.